Journal of Controlled Release 386 (2025) 114166

Contents lists available at ScienceDirect

Journal of Controlled Release

journal homepage: www.elsevier.com/locate/jconrel

Ultra-long-acting injectable, biodegradable, and removable in-situ forming implant with cabotegravir for HIV prevention

Thy Le [a], Isabella C. Young [b], Jasmine L. King [a], Mackenzie L. Cottrell [c], Amar Shankar Kumbhar [d], Craig Sykes [c], Amanda Schauer [c], Gabriela De la Cruz [e], Caleb T. Kozuszek [d], Nanditha Chundayil Kalathil [a], Alexandra Abel [a], Rani S. Sellers [f,g], Angela D.M. Kashuba [c], S. Rahima Benhabbour [a,b,*]

[a] Lampe Joint Department of Biomedical Engineering, North Carolina State University and The University of North Carolina at Chapel Hill, Chapel Hill, NC, USA
[b] Division of Pharmacoengineering and Molecular Pharmaceutics, UNC Eshelman School of Pharmacy, University of North Carolina at Chapel Hill, Chapel Hill, NC, USA
[c] Division of Pharmacotherapy and Experimental Therapeutics, UNC Eshelman School of Pharmacy, University of North Carolina at Chapel Hill, Chapel Hill, NC, USA
[d] Department of Chemistry, University of North Carolina at Chapel Hill, Chapel Hill, NC, USA
[e] Lineberger Comprehensive Cancer Center, University of North Carolina at Chapel Hill, Chapel Hill, NC, USA
[f] Department of Pathology and Laboratory Medicine, University of North Carolina at Chapel Hill, Chapel Hill, NC, USA
[g] Division of Comparative Medicine, University of North Carolina at Chapel Hill, Chapel Hill, NC, USA

ARTICLE INFO

Keywords:
In-situ forming implants
HIV prevention
Injectable
Ultra-long-acting
X-ray imaging
Cabotegravir

ABSTRACT

HIV is a global health issue affecting approximately 40 million people worldwide, with low patient adherence being the primary challenge for maintaining effective pre-exposure prophylaxis (PrEP). Limitations of oral PrEP are mainly attributed to lack of adherence due to pill fatigue or stigma [1, 2]. Recently introduced long-acting injectables offer several advantages over daily PrEP, namely by improving adherence and improving efficacy [3–5]. The approved long-acting injectable Apretude® is administered every two months and elicits a long pharmacokinetic tail of >15 months that can lead to potential drug-resistant virus [6]. To address these limitations, we report on an ultra-long-acting injectable cabotegravir/barium sulfate (CAB/$BaSO_4$) in-situ forming implant (ISFI) capable of maintaining therapeutic CAB concentrations (> 4× PA-IC_{90}) for up to 390 days. In this work, we optimized the ISFI formulation to include a contrast agent, $BaSO_4$, to assess in vivo depot visualization and migration using X-ray imaging. CAB/$BaSO_4$ ISFIs were investigated in vitro to determine CAB release kinetics, and in vivo to assess safety and pharmacokinetics in BALB/c mice. The CAB/$BaSO_4$ ISFI was well-tolerated and showed minimal to moderate signs of local inflammation and none to minimal systemic inflammation. At 24 hours post removal of the CAB/$BaSO_4$ ISFI, CAB plasma concentrations reached below the 1 × PA-IC_{90} benchmark and below the limit of quantification within 14 days for 5 out of 6 mice. A full biodistribution study showed that CAB was mainly localized at the injection site subcutaneous tissue and plasma, with no detectable concentrations in other organs. Whole-body X-ray imaging showed that implants were visible for up to 268 days post administration with no noticeable migration. This is the first report of a CAB/$BaSO_4$ ISFI that is imageable, ultra-long-acting (>180 days), biodegradable, and removable, that can potentially revolutionize current HIV PrEP and help curb the global HIV epidemic.

1. Introduction

Despite effective antiretroviral therapy, HIV remains a global health challenge, affecting approximately 39.9 million people worldwide and causing over 630,000 AIDS-related deaths in 2023 [7,8]. If HIV is left untreated, the virus can progressively destroy the immune system, leading to acquired immunodeficiency syndrome (AIDS) [9]. Over the past few decades, medical research and pharmaceutical development have significantly transformed HIV into a manageable chronic condition. Despite significant advancements, the virus's persistent spread

* Corresponding author at: Lampe Joint Department of Biomedical Engineering, North Carolina State University and The University of North Carolina at Chapel Hill, Chapel Hill, NC, USA.
E-mail address: benhabs@email.unc.edu (S.R. Benhabbour).

https://doi.org/10.1016/j.jconrel.2025.114166
Received 7 May 2025; Received in revised form 22 July 2025; Accepted 23 August 2025
Available online 25 August 2025

with an estimated 1.3 million new infections in 2023 requires focus on effective prevention strategies [8,10].

Effective pre-exposure prophylaxis (PrEP) is critical to protect high-risk individuals [11], alleviate socioeconomic pressures [12], and interrupt the cycle of transmission [13], particularly in high-prevalence regions such as Sub-Saharan Africa, which accounts for nearly half of the global new infections in 2023 [8]. Early prevention methods relied on condoms and behavioral education, achieving modest success but faltering due to inconsistent adherence [14,15]. With the introduction of Truvada® and Descovy® as daily oral PrEP, HIV acquisition risk was reduced by up to 99 % and demonstrated comparable efficacy when taken consistently [16,17]. However, the effectiveness of oral PrEP remains a significant hurdle due to difficulties in maintaining daily adherence to medication [1,2,18,19].

To ease the adherence burden, there has been a general shift towards therapies that require less frequent dosing. In 2021, the FDA approved long-acting injectables Apretude® for HIV PrEP and Cabenuva® for treatment [3,20]. Apretude, a long-acting injectable containing Cabotegravir (CAB), was shown to reduce HIV incidence by 69 %–90 % compared to oral PrEP with just six administrations per year [3,4,5]. Cabenuva, administered as two long-acting injectables containing CAB and Rilpivirine (RPV), was shown to sustain viral suppression in HIV-positive individuals, offering a potent dual-drug regimen for HIV treatment [20,21]. Both formulations leverage CAB's potency (4× PA-IC90 of 664 ng/mL) and simplify dosing, but they elicit injection-site reactions (81 %–85 % incidence) and elicit a long pharmacokinetic (PK) tail for over 15 months after the final dose. This PK tail raises concerns about potential breakthrough infections and emerging drug resistance [3,4,6]. Given these limitations, there remains a clear need to develop long-acting treatments that retain CAB's efficacy yet shorten the PK tail, thereby improving both adherence and resistance management in PrEP regimens.

To address these limitations, our research group has developed ultra-long-acting in-situ forming implants (ISFIs) that have the potential to reduce dosing frequency to just 1–2 times a year [22–24]. Moreover, these ISFIs are biodegradable and can be removed to terminate treatment if required, which reduces adverse reactions and eliminates the long PK tail associated with other long-acting treatments to further reduce the risk of breakthrough infections or drug-resistant virus [22–24]. Importantly, ISFIs are subcutaneously injected to enable potential self-administration and increase adherence and accessibility for patients. We previously developed an ultra-long-acting formulation of CAB for PrEP that can release CAB at protective plasma and tissue concentrations for more than six months and was well tolerated in both mice and macaque models [23]. Our CAB ISFI technology incorporates a poly(lactic-*co*-glycolic acid) (PLGA) biodegradable polymer, dimethyl sulfoxide (DMSO), and *N*-methyl-2-pyrrolidone (NMP) as water-miscible organic solvents, with CAB as the active pharmaceutical ingredient (API). Upon subcutaneous (SC) injection, the suspension undergoes a phase inversion that occurs through the exchange between the water-miscible organic solvents within the formulation and the aqueous body fluids within the tissue environment [25], creating a porous solid or semi-solid depot with CAB entrapped within the precipitated polymer matrix. After this initial burst release, CAB can then be released from the depot into systemic circulation through diffusion and polymer degradation mediated mechanisms.

A major barrier to the broad implementation of long-acting injectables is the difficulty of confirming depot location and retrieving the formulation in cases where treatment needs to be suspended. To address this, we focused on improving the ISFI by integrating barium sulfate ($BaSO_4$), a common contrast agent for X-ray imaging, into the formulation to make it radiopaque and surgically retrievable when necessary. $BaSO_4$ has already been clinically approved for subcutaneous use in products like NEXPLANON®, which maintains pharmacokinetic bioequivalence to IMPLANON® while providing reliable X-ray visibility for straightforward localization and removal [26]. Beyond implants, $BaSO_4$ has also been added to polyurethane catheters (ARROW® PICC, Cook® Turbo-Ject PICC, etc.) [27–29] and bone cements (Simplex P®, KyphX® HV-R™, etc.) [30,31]. Although a CT-visible ISFI has been previously reported utilizing the iodinated agent iohexol [32], the water-soluble agent can leach out thus diminishing long-term signal and potentially accelerating PLGA degradation by hydrolysis. Since the use of $BaSO_4$ has been validated across multiple devices and has been shown to not alter drug release kinetics, we selected $BaSO_4$ as the radiopaque agent for our ISFI formulation. Herein, we investigated in vivo depot visualization and migration, by integrating $BaSO_4$ into the formulation to allow for non-invasive localization of the depot, facilitate its retrieval, and monitor potential implant migration. We developed and characterized the performance of CAB ISFIs formulated with different weight percentages of $BaSO_4$ to determine the concentration of $BaSO_4$ in the ISFI formulation that does not adversely affect the in vitro and in vivo release of CAB. In vivo studies showed that the CAB/$BaSO_4$ ISFIs elicited a similar PK profile to the CAB-only ISFI, demonstrating that the inclusion of $BaSO_4$ did not significantly alter the formulation performance. We conducted a long-term (268 days) X-ray imaging study using BALB/c mice to assess and confirm the radiopacity of the various CAB/$BaSO_4$ ISFI formulations. We also analyzed the PK tail post-depot removal at day 180 post ISFI administration. Our findings demonstrate that the addition of barium sulfate to the CAB ISFI formulation allows for in vivo visualization of the depots and ease of depot removal, while maintaining therapeutic plasma CAB concentration in mice for up to 390 days. This work advances on prior studies as we extend the duration of the CAB ISFI from 180 days to 390 days with a radiopaque depot, while demonstrating a short PK tail post depot removal and no visible migration of the depots over 268 days in mice.

2. Materials and methods

2.1. Reagents and materials

50:50 poly(DL-lactide-*co*-glycolide) (PLGA) was purchased from LACTEL (Birmingham, AL, Part #: B6017-1G, Lot #A21–030, molecular weight (MW) 10 kDa, viscosity range: 0.15–0.25 dL/g). *N*-methyl-2-pyrrolidone (NMP, USP) was received from ASHLAND (Wilmington, DE, Product code 851263, 100 % NMP). Dimethyl sulfoxide (DMSO, ≥99.9 %) was purchased from VWR Chemicals (Radnor, PA; Cat. No. BDH1115-4LP; Lot No. 040811B). Solutol-HS 15, phosphate buffered saline (0.01 M PBS, pH 7.4), and HPLC grade acetonitrile (ACN) and water were purchased from Sigma Aldrich (St. Louis, MO). For in vitro release studies, Cabotegravir (CAB) was purchased from Advanced ChemBlocks Inc. (Burlingame, CA; Cat. No. L21808). For in vivo studies, high purity (≥99.7 %) CAB was purchased from Selleckchem (Houston, TX, Cat. No. S7766), and sterile filtered DMSO (≥99.9 %) was purchased from Fisher Scientific (Fairlawn, NJ; Cat. No. BP231–100; Lot No. 234276). Barium sulfate ($BaSO_4$) was purchased from Spectrum Chemical MFG. Corp. (Gardenia, CA, and New Brunswick, NJ; Cat. No. 2KJ0029). 98.5 % acrylamide (AM) and ammonium persulfate (APS) were purchased from Acros Organics (Carlsbad, CA; AM Cat. No. 16435000; APS Cat. No. 40116–1000), and 2 % bis-acrylamide solution and *N*, *N*, *N*′, *N*′-tetramethyl ethylenediamine (TEMED) were purchased from Fisher Scientific (Hampton, NJ; bis-acrylamide Cat. No. BP150–20, TEMED Cat. No. BP1404–250).

2.2. Methods

2.2.1. High performance liquid chromatography (HPLC)

A reverse-phase HPLC analysis was carried out on an Agilent 1260 HPLC system (Agilent Technologies, Santa Clara, CA, USA) equipped with a Diode Array Detector, and an LC pump with autosampler. The stationary phase utilized for the analysis of CAB was an Inertsil ODS-3 column (4 μm, 4.6 × 150 mm, 100 Å, GL Sciences, Torrance, CA) that was maintained at 40 °C. Chromatographic separation was achieved by

gradient elution using a mobile phase consisting of 0.1 % trifluoroacetic acid in water and acetonitrile (H_2O/ACN 95:5 *v*/v). The flow rate was set at 1.0 mL/min, and the total run time was 25 min for each 25 μL injection. CAB was detected at 254 nm.

2.2.2. Preparation of ISFI formulations

A homogeneous placebo solution was created by mixing 50:50 PLGA (MW: 10 kDa) with a 1:1 NMP: DMSO solution at a 1:4 w/w ratio in a 7 mL scintillation vial at room temperature. $BaSO_4$ was added at concentrations of 0.1, 1, 5, and 10 % w/w to the placebo solution. CAB was then added to achieve a target drug loading of 500 mg/mL in a stable suspension above its saturation solubility (167.12 ± 12.04 mg/mL in 1:1 NMP:DMSO) [23]. Formulation homogeneity was determined by quantifying CAB concentration using HPLC analysis, with formulations deemed homogeneous if the standard deviation associated with the average concentration in all sample aliquots was ≤5 %. For in vivo studies, ISFI formulations were prepared under aseptic conditions in a biosafety cabinet. All solvents and the ISFI placebo were sterile filtered using a 0.2 μm sterile filter.

2.2.3. In vitro cumulative drug release

In vitro drug release was performed similarly to methods previously described [22–24]. Drug release kinetics of CAB/$BaSO_4$ ISFIs were investigated by injecting 30 mg ± 3 mg of the ISFI formulation into 100 mL of release medium (0.01 M PBS, pH 7.4, with 2 % Solutol) and incubating at 37 °C under sink conditions. Solutol was used to enhance drug solubility and maintain sink conditions, defined as a drug concentration at or below one-fifth of its maximum solubility in PBS with 2 % Solutol [33]. Sample aliquots (1 mL) were collected at predetermined time points. The release medium was completely removed and replaced with 100 mL of fresh medium every week to maintain sink conditions. The drug concentration in the release medium was determined by HPLC. Cumulative drug release was calculated from the HPLC analysis and normalized by the total mass of the drug in the implant. All experiments were performed in triplicate. The percent depot mass loss overtime was calculated based on the equation: $\frac{M_0 - M_t}{M_0} \times 100\%$, where M_0 is the initial weight of the ISFI injected into the medium and M_t is the final dry weight of the depot at time *t*.

2.2.4. Scanning electron microscopy (SEM) imaging with energy dispersive X-ray analysis (SEM-EDX)

Implant microstructures were evaluated by scanning electron microscopy (SEM) as previously described [22,24,34], combined with energy dispersive X-ray spectroscopy (EDX). Depots were formed upon injecting 30 ± 3 mg of CAB and CAB/$BaSO_4$ ISFI formulations (500 mg/mL) into 100 mL of 0.01 M PBS (pH 7.4) with 2 % Solutol at 37 °C. Depots were retrieved at 3, 30, 60-, 90-, 120-, and 180-days post-incubation, flash-frozen with liquid nitrogen, and lyophilized for 48 h (FreeZone Benchtop Freeze Dryer, Labconco, Kansas City, MO). The freeze-dried depots were stored at −20 °C until imaging. After collection, the depots were bisected with a handheld razor, mounted on an aluminum stub using carbon tape, and the exposed cross-section was sputter coated with a 6–7.5 nm gold-palladium alloy (60:40) (Cressington 108 auto Sputter Coater, Cressington Scientific Instruments Ltd., Watford, UK). The coated samples were then imaged using a Hitachi Model S-4700 Field Emission Scanning Electron Microscope at an acceleration voltage of 20.0 kV and a 12.2 mm working distance (Hitachi High-Tech Corporation, Tokyo, Japan). Elemental composition was analyzed using an EDX system.

2.2.5. Accelerated stability studies and post-storage in vitro drug release

Stability studies were performed similarly to previously described procedures [23]. CAB/$BaSO_4$ ISFI formulations were stored in sealed glass vials placed in a Binder Model KBF 240 constant climate chamber at 40 °C and 75 % relative humidity (RH). Formulations were removed at 30- and 90-days post-storage, and sample aliquots (1–4 mg, $n = 3$) were collected and analyzed by HPLC to assess drug content and potential drug degradation. A post-storage in vitro release study was conducted if the formulation demonstrated physical stability (i.e., no discoloration or phase separation), contained drug concentration similar to time 0 control formulation (<10 % difference), and deemed as a homogeneous suspension by HPLC analysis. Post-storage release was performed by injecting 30 mg ± 3 mg of the ISFI formulation into 100 mL of release medium (0.01 M PBS, pH 7.4, with 2 % Solutol) and incubating at 37 °C under sink conditions.

2.2.6. Density measurement

The density of CAB/$BaSO_4$ ISFIs was measured as previously reported [22,24]. Briefly, the density was determined by weighing 1 mL of the formulation suspension in a 1 mL volumetric flask.

2.2.7. Preparation and injection into polyacrylamide hydrogels

The injectability of CAB/$BaSO_4$ ISFIs was evaluated as previously reported [23]. An injection volume of 1 mL was done in vitro to simulate the injection volume administered to non-human primates. The preparation of polyacrylamide hydrogels (40 mL) was adapted from previous protocols [35,36]. This involved sequentially adding 40 wt% acrylamide (AM) aqueous solution, 2 wt% bis(acrylamide) (BisAM) aqueous solution, 10 wt% ammonium persulfate (APS) aqueous solution, and 50 μL *N*,*N*,*N*′,*N*′-tetramethyl ethylenediamine (TEMED) and incubating at 4 °C overnight to allow polymerization. The polyacrylamide hydrogels were subsequently submerged in 0.01 M PBS, pH 7.4, with 2 % Solutol until equilibrium swelling was reached. A 1 mL sample of CAB/$BaSO_4$ ISFI was injected into the hydrogel using a 16, 18, or 19G needle to assess injectability.

2.2.8. In vivo X-ray imaging study

An in vivo X-ray imaging study was conducted to assess the visibility and migration of CAB/$BaSO_4$ ISFIs in female BALB/c mice (16–20 weeks, Jackson Laboratory). All experiments were performed under an approved protocol by the University of North Carolina Animal Care and Use Committee. Placebo and CAB-loaded ISFI formulations were prepared with various concentrations of $BaSO_4$ (1, 5, 10 wt%), a contrast agent for X-ray imaging. Mice received a 50 μL subcutaneous injection of each formulation using a 19G needle ($n = 3$ mice per group, $n = 15$ mice total). Placebo formulations were injected into the left flank as a control, and CAB/$BaSO_4$ ISFI formulations were injected into the right flank. Full-body X-ray images were collected at days 3, 7, 14, 30 and biweekly thereafter post-ISFI administration. At predetermined timepoints, mice (n = 3 mice per group) were euthanized, and depots were retrieved via a small skin incision at the injection site to quantify depot degradation using gel permeation chromatography (GPC) analysis.

2.2.9. In vivo safety studies

A 180-day in vivo study was conducted to assess the local and systemic inflammation of CAB and CAB/$BaSO_4$ ISFIs in female BALB/c mice (16–20 weeks, Jackson Laboratory). All experiments were performed under a protocol approved by the University of North Carolina Animal Care and Use Committee. Mice were subcutaneously injected with 50 μL of either CAB ISFI or CAB with 10 % $BaSO_4$ ISFI formulation using a 19G needle ($n = 25$ mice per group). Ten mice did not receive any injection and served as the control group. At 7, 30-, 60-, 90-, and 180-days post ISFI administration, mice were euthanized ($n = 5$ per timepoint for treatment groups and n = 2 per timepoint for the control group), and blood samples were collected via heart puncture into capillary tubes, then stored at −80 °C. Tumor necrosis factor-alpha (TNF-α) and interleukin-6 (IL-6) proinflammatory cytokines were quantified by enzyme-linked immunosorbent assay (ELISA, MAX™ Deluxe sets, BioLegend®). The depot and the surrounding skin were circumferentially excised along with the subjacent subcutaneous adipose tissue to assess local inflammation via histology. The specimen was placed in 10 %

neutral buffered formalin at a ratio of 1:10 tissue to fixative at room temperature for 72 h, then transferred to 70 % ethanol at room temperature until specimen grossing. Fixed skin specimens were trimmed through the middle with the depot centrally oriented, the cut skin was processed and then embedded on-edge into paraffin blocks. Samples were sectioned at 4 μm and stained with Hematoxylin and Eosin using the autostainer XL from Leica Biosystems. The sections were stained with Hematoxylin (Richard-Allen Scientific, 7211) for 2 min and Eosin-Y (Richard-Allen Scientific, 7111) for 1 min. Clarifier 2 (7402) and Bluing (7111) solutions from Richard-Allen Scientific were used to enhance the reaction. Inflammation was scored by a board-certified veterinary pathologist as follows: 0: no inflammation; 1: minimal inflammation characterized by low numbers of scattered inflammatory cell infiltrates around the depot; 2: mild inflammation, characterized by scattered inflammatory cells and small aggregates of inflammatory cells around and/or within the depot; 3: moderate inflammation, characterized by aggregates of inflammatory cells around and/or within the depot and beginning to extend beyond the region of the depot; 4: marked inflammation, characterized by dense aggregates of inflammatory cells around and/or within the depot, as well as extending into the surrounding subcutis and dermis; 5: severe inflammation, characterized by infiltrating inflammatory cells around and or within the depot which is associated with extensive tissue destruction in the dermis and subcutis around the depot.

2.2.10. In vivo pharmacokinetics (PK) studies

2.2.10.1. Time to completion PK study. A time-to-completion (TTC) in vivo study was conducted to assess the drug release kinetics of CAB/$BaSO_4$ ISFIs (1250 mg/kg CAB) in female BALB/c mice (8–10 weeks, Jackson Laboratory). All experiments involving mice were performed under a protocol approved by the University of North Carolina Animal Care and Use Committee. Mice were subcutaneously injected with 50 μL of the 10 % $BaSO_4$ CAB ISFI formulation using a 19G needle ($n = 6$ mice per group). Peripheral blood was collected at 1 h, 3 h, 1 day, 3 days, 7 days, 14 days, 30 days, and subsequent monthly timepoints post-ISFI administration into capillary tubes coated with EDTA to isolate plasma, continuing for up to 480 days until plasma CAB concentration reached below limit of quantification (BLOQ).

2.2.10.2. Post depot removal PK tail study. To assess the PK tail post depot removal (PDR), 12 female BALB/c mice (8–10 weeks, Jackson Laboratory) were injected with 50 μL of the CAB/$BaSO_4$ formulation. Depots were removed via a small skin incision at the injection site at day 180 post ISFI administration, and plasma samples were collected at days 1, 7, 14, and 30 post depot removal ($n = 6$ mice per timepoint). At the PDR study completion, the remaining mice (n = 6) were euthanized to collect tissues and organs to investigate CAB biodistribution. All samples were stored at −80 °C until further pharmacokinetics analysis. Depots retrieved post euthanasia were analyzed to quantify polymer degradation using GPC analysis ($n = 3$) and to quantify residual drug by HPLC analysis (n = 3). To quantify residual drug concentration, excess tissue was carefully removed, and depots were subsequently dissolved in acetonitrile, and residual drug concentration was quantified using HPLC analysis. The percent residual drug was calculated based on the equation: $\frac{CAB_t}{CAB_0} \times 100\%$, where CAB_0 is the amount of CAB determined from the initial ISFI volume injected and CAB_t is the CAB remaining in the depot at time t.

2.2.11. In vivo biodistribution studies

An in vivo full biodistribution study was conducted in female BALB/c mice to assess the biodistribution of CAB throughout the body (plasma, SC tissue and organs). All experiments were performed under a protocol approved by the University of North Carolina Animal Care and Use Committee. Mice were subcutaneously injected with 50 μL of either CAB ISFI ($n = 5$ mice per timepoint) or CAB with 10 % $BaSO_4$ ISFI ($n = 6$). At day 30, 60, 90, and 180 post ISFI administration, mice injected with CAB ISFI were euthanized to collect plasma, organs, and injection site tissue for CAB concentration analysis. Similarly, at day 180 post administration, mice injected with CAB/$BaSO_4$ ISFI were euthanized to assess CAB biodistribution in blood, injection site tissue and organs. Collected organs and tissues included injection site subcutaneous tissue, cervical, axillary, and inguinal lymph nodes, cervix, rectum, vagina, duodenum, ileum, colon, liver, and spleen. All samples were stored at −80 °C until further analysis. CAB was extracted from mouse plasma by either protein precipitation or liquid extraction with the stable, isotopically labeled internal standard, $^{13}C,^{2}H_2,^{15}N$-CAB before analysis by LC-MS/MS. Chromatographic separation was performed on a Waters Atlantis T3 (50 × 2.1 mm, 3 mm particle size) analytical column under gradient conditions with detection in positive ion electrospray mode on an AB Sciex API-5000 triple quadruple mass spectrometer. The lower limit of quantitation for the plasma assay was 6.25 ng/mL. Calibration standards and quality control samples were within 25 % of nominal concentrations. Weighed tissues were transferred into Precellys® hard tissue reinforced metal bead kit tubes (Cayman Chemical Company) containing 1 mL of 70:30 acetonitrile:water, homogenized then centrifuged. Following protein precipitation extraction with the isotopically labeled internal standard, $^{13}C,^{2}H_2,^{15}N$-CAB, CAB was separated using reverse-phase chromatography via a Waters Atlantis T3 (50 × 2.1 mm, 3 μm particle size) analytical column. An AB Sciex API-5000 triple quadruple mass spectrometer was used to detect the analyte and internal standard under positive ion electrospray conditions. The lower limit of quantitation for the tissue assay was 0.500 ng/mL. Precision and accuracy of the calibration standards and quality control samples were within 20 % of nominal concentrations. By assuming a tissue density of 1 g/mL [37], final tissue concentrations were normalized to tissue mass and reported in ng/g.

2.2.12. Gel permeation chromatography (GPC)

GPC analysis was utilized to evaluate polymer degradation of CAB and CAB/$BaSO_4$ ISFIs both in vitro and in vivo, as previously described [23,34]. From in vitro studies, polymer degradation was quantified for formulations stored at 4 °C and 40 °C /75 % RH for 367 days, for depots collected from the post-storage in vitro drug release study, and for depots incubated in release media (PBS pH 7.4) for 3, 30, 60, 90, 120, and 180 days. Depots were flash-frozen with liquid nitrogen and lyophilized for 48 h. Additionally, depots retrieved from in vivo studies post euthanasia at days 30, 60, 90, and 180 post ISFI administration were analyzed by GPC to assess polymer degradation. Both in vitro and in vivo depots (CAB, CAB/$BaSO_4$ ISFIs) as well as neat polymer (10 kDa PLGA) were analyzed using a Tosoh Biosciences EcoSEC Elite HLC-8420 equipped with a TSKgel GMH-M column. Molecular weight determination was conducted relative to polystyrene standards and measured via refractive index (RI) detection.

2.2.13. Statistical analysis

A repeated-measures two-way ANOVA test and a Tukey's multiple comparisons test was performed with respect to timepoint and formulation to analyze differences in the following studies: (1) to compare in vitro drug release of CAB/$BaSO_4$ ISFIs with varying barium sulfate concentrations, (2) to compare in vitro PLGA MW degradation between CAB and CAB/$BaSO_4$ ISFIs, (3) to compare in vitro post-storage release studies and post storage PLGA MW degradation compared to baseline (time 0 release and PLGA MW), (4) to compare in vivo systemic inflammation (TNF-α and IL-6 concentrations in plasma) to the no injection control group, (5) to compare CAB and CAB/$BaSO_4$ ISFI in vivo plasma concentrations, and (6) to compare CAB and CAB/$BaSO_4$ ISFI in vivo drug biodistribution. Statistical analyses were performed in GraphPad Prism 9 (GraphPad Software, Inc., La Jolla, CA, USA). For all statistical tests, a p value of <0.05 was considered significant (95 % confidence level).

3. Results

3.1. Development of the CAB/$BaSO_4$ ISFI

In our efforts to develop a radiopaque ISFI, we incorporated barium sulfate ($BaSO_4$) into our previously established CAB ISFI formulation [23]. The standard CAB ISFI formulation consists of a stable suspension of 500 mg/mL CAB in 1:4 w/w PLGA (50:50, 10 kDa):(NMP: DMSO). Our primary goal was to ensure that the addition of $BaSO_4$ would not adversely affect the drug loading and drug release kinetics from the ISFI in vitro and in vivo. To evaluate the impact of $BaSO_4$ addition, we conducted cumulative in vitro release studies on four different CAB/$BaSO_4$ ISFI formulations, comparing them to the standard CAB ISFI formulation over 30 days. Results (Fig. 1A,D) demonstrated that the inclusion of $BaSO_4$ did not affect the drug loading capacity (Fig. 1D) or the initial burst release of CAB (Fig. 1A).

Cumulative in vitro release of CAB formulated with 0.1, 1, 5, and 10 % $BaSO_4$ elicited significantly lower release rates ($p < 0.001$) at day 30 compared to CAB-only ISFIs, and burst release decreased with increasing $BaSO_4$ concentration in the formulation (Fig. 1A,D). Despite these differences, all CAB/$BaSO_4$ ISFI formulations maintained sustained drug release over 30 days and were projected to release CAB for more than 6 months in vitro. Moreover, the effect of $BaSO_4$ was not as evidenced in vivo until past day 180 where a similar effect was observed with the CAB/$BaSO_4$ ISFI eliciting significantly lower plasma CAB concentrations compared to CAB ISFIs.

It is worth noting that the incorporation of $BaSO_4$ resulted in a different PLGA to CAB ratio within the formulation. For the standard CAB ISFI formulation, PLGA:CAB ratio was 1:3.5 w/w compared to 1:4.2 w/w in the CAB/$BaSO_4$ ISFI, indicating a lower concentration of PLGA in the CAB/$BaSO_4$ ISFIs. Despite this change in ratio, the CAB loading remained similar for both the CAB/$BaSO_4$ ISFI and the standard CAB ISFI formulations, as evidenced by the comparable amounts of CAB present in each formulation (Fig. 1C). This similar drug loading resulted in similar release of CAB within the first 7 days for all the formulations analyzed (Fig. 1A, B). By day 30, the overall release rate of CAB decreased significantly for all formulations containing $BaSO_4$ compared to the standard CAB ISFIs which was attributed to the hydrophobic nature of $BaSO_4$ which could result in reduced water influx and slowed depot degradation, hence reducing drug release kinetics. Moreover, the inclusion of $BaSO_4$ elicited an increase in formulation viscosity and density, which in turn can affect the degradation rate of PLGA. This change is evident in the increasing viscosity of the formulation with increased $BaSO_4$ concentration and the increase in density at 1.297 g/mL vs 1.215 g/mL for CAB/$BaSO_4$ and standard CAB ISFI formulations respectively (Supplementary Fig. 1).

The CAB/$BaSO_4$ ISFI was used to assess in vivo depot visualization and migration using non-invasive full-body X-ray imaging. Given the increased formulation viscosity in the presence of $BaSO_4$, we first assessed the practical injectability of the formulation to ensure effective in vivo administration. We successfully injected 1 mL of the CAB/$BaSO_4$ formulation into subcutaneous tissue-mimicking hydrogels using an 18G needle (Supplementary Fig. 1). Following this, an in vivo X-ray imaging study was conducted to evaluate the visualization and potential migration of the ISFI over time (Fig. 1C, Supplementary Fig. 2, Supplementary Fig. 3). Results demonstrated that $BaSO_4$ enhanced implant visibility under X-ray in a concentration-dependent manner, with the ISFI formulation containing 10 % $BaSO_4$ yielding the brightest signal. Additionally, there was no apparent migration of the implants over the study duration, confirming predictable implant localization at the injection site. Based on the initial results from the 5 % and 10 % $BaSO_4$ formulations, the in vivo X-ray imaging study was extended to

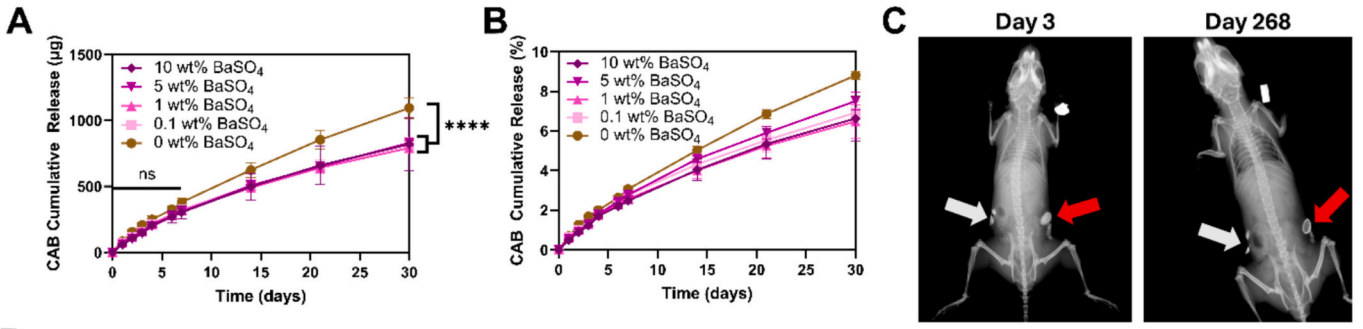

D

Formulation: 500 mg/mL 1:4 PLGA (10 kDa):Solvent (1:1 NMP:DMSO)	CAB Analytical Loading (mg/mL)	Burst Release (24h) (µg)	Burst Release (24h) (%)	Cumulative Release at 30 days (%)	Release rate (µg/day)	Projected duration to 100% release (days)
0 wt% $BaSO_4$	504.4±26.6	85.5±9.4	0.69±0.04	8.80±0.18	35.47	362
0.1 wt% $BaSO_4$	510.3±4.7	75.4±10.0	0.64±0.07	6.92±0.60	31.98	368
1 wt% $BaSO_4$	501.8±17.2	76.3±5.03	0.62±0.07	6.48±0.84	31.34	380
5 wt% $BaSO_4$	500.0±12.1	62.0±8.6	0.56±0.05	7.50±0.45	32.14	345
10 wt% $BaSO_4$	505.9±4.2	59.6±7.53	0.49±0.04	6.63±1.13	32.02	384

Fig. 1. CAB/$BaSO_4$ ISFI in vitro release kinetics. All in vitro release studies were done in phosphate buffer saline (PBS, pH 7.4 with 2 % solutol) at 37 °C under sink conditions. A) Cumulative release (µg) of CAB/$BaSO_4$ formulations with varying concentration of barium sulfate. Statistical analysis: two-way ANOVA with Tukey's multiple comparisons comparing CAB release with respect to formulation and timepoint (ns = no significance; ****$p < 0.0001$). B) Cumulative release (%) of CAB/$BaSO_4$ formulations with varying concentration of barium sulfate. C) X-ray images of a female BALB/c mouse injected with CAB +10 wt% $BaSO_4$ ISFI (red arrow) and Placebo +10 wt% $BaSO_4$ ISFI (white arrow). D) Summary table of release kinetics for CAB/$BaSO_4$ ISFI formulations. The cumulative mass of CAB (M, µg) released at time t (days) fits the zero-order equation $M(t) = kt$ where k is the experimentally determined slope and release rate (µg/day). Because no drug is present in the medium at $t = 0$, the intercept was fixed at zero. For each formulation, we performed a least-squares linear regression on the in vitro data ($R^2 > 0.97$ for all fits). Thus, the projected duration (T_p) required to exhaust the total loaded drug mass (M_0) can be calculated with the equation $T_p = \frac{M_0}{k}$. (For interpretation of the references to colour in this figure legend, the reader is referred to the web version of this article.)

determine the longevity of the radiopacity signals. During the whole monitoring period, the radiopacity signal of ISFIs containing 10 % $BaSO_4$ remained constant, and no new radiopaque signals were detected in adjacent tissues or organs (Supplementary Fig. 2). Compared to the placebo only depots, CAB/$BaSO_4$ depots retained ~10 % extra mass (Supplementary Fig. 3C), indicating minimal $BaSO_4$ loss. Despite challenges related to aging mice and equipment issues, the study confirmed that depots containing 10 % $BaSO_4$ remained visible under X-ray for at least 268 days, showing the potential of the formulation for long-term monitoring. Ultimately, the 10 % $BaSO_4$ formulation was selected as the optimized formulation for future studies due to its superior X-ray visibility.

3.2. *In vitro degradation of CAB/$BaSO_4$ ISFI*

To corroborate the in vitro release and in vivo X-ray imaging studies, we investigated the degradation and change in depot microstructure over time for the CAB/$BaSO_4$ and standard CAB ISFI formulations. SEM images of the CAB/$BaSO_4$ and CAB ISFI microstructures were assessed to understand how the physical properties of each formulation relate to the in vitro drug release kinetics and depot radiopacity. SEM images captured at various timepoints over 180 days provided a detailed view of the microstructures for both the CAB and CAB/$BaSO_4$ ISFI formulations. Both formulations resulted in depots with dense, low porosity microstructures due to high drug loading (41 % w/w CAB). This structural characteristic aligns with the similar initial release rates observed in the in vitro drug release studies. After 30 days, polymer degradation becomes a significant contributing mechanism to drug release as reported in our previous studies with this ISFI system [34]. This was observed in both the CAB and CAB/$BaSO_4$ ISFIs which elicited noticeable decrease in depot size, with no visual differences in their microstructural degradation patterns (Supplementary Fig. 4 and 5). However, the CAB/$BaSO_4$ ISFI elicited the presence of white particulate matter, dispersed among the drug crystals (Fig. 2A, Supplementary Fig. 5 and 6B), which was identified as $BaSO_4$ using EDX analysis. The $BaSO_4$ particles were dispersed within the drug crystals, thus resulting in a denser polymer-drug matrix. The densely packed microstructure of the CAB/$BaSO_4$ depots further supports the slower decrease ($p = 0.0025$) in PLGA MW observed with CAB/$BaSO_4$ (34 % at day 180) compared to the CAB ISFI (~44 % at day 180) (Fig. 2A), resulting in less diffusion pathways with insoluble $BaSO_4$ physically blocking water influx that can facilitate PLGA degradation via hydrolysis. To further confirm the elemental composition of the drug crystals and $BaSO_4$, SEM-EDX was conducted (Supplementary Fig. 6 and 7). CAB was identified through the presence of the element fluorine and $BaSO_4$ was identified through the presence of the elements barium and sulfur. These analyses validated the presence and distribution of $BaSO_4$ within the CAB/$BaSO_4$ ISFI formulations, confirming the components within the polymer matrix.

3.3. *Stability and post-storage in vitro release studies*

To determine the shelf-life of the CAB/$BaSO_4$ ISFI, we performed stability studies at two different storage conditions (4 °C and 40 °C/75 % RH). Post-storage in vitro release kinetics were conducted after 30 and 90 days of storage under the aforementioned storage conditions. After 30 days at 4 °C and 40 °C/75 % RH and 90 days at 4 °C, there were no

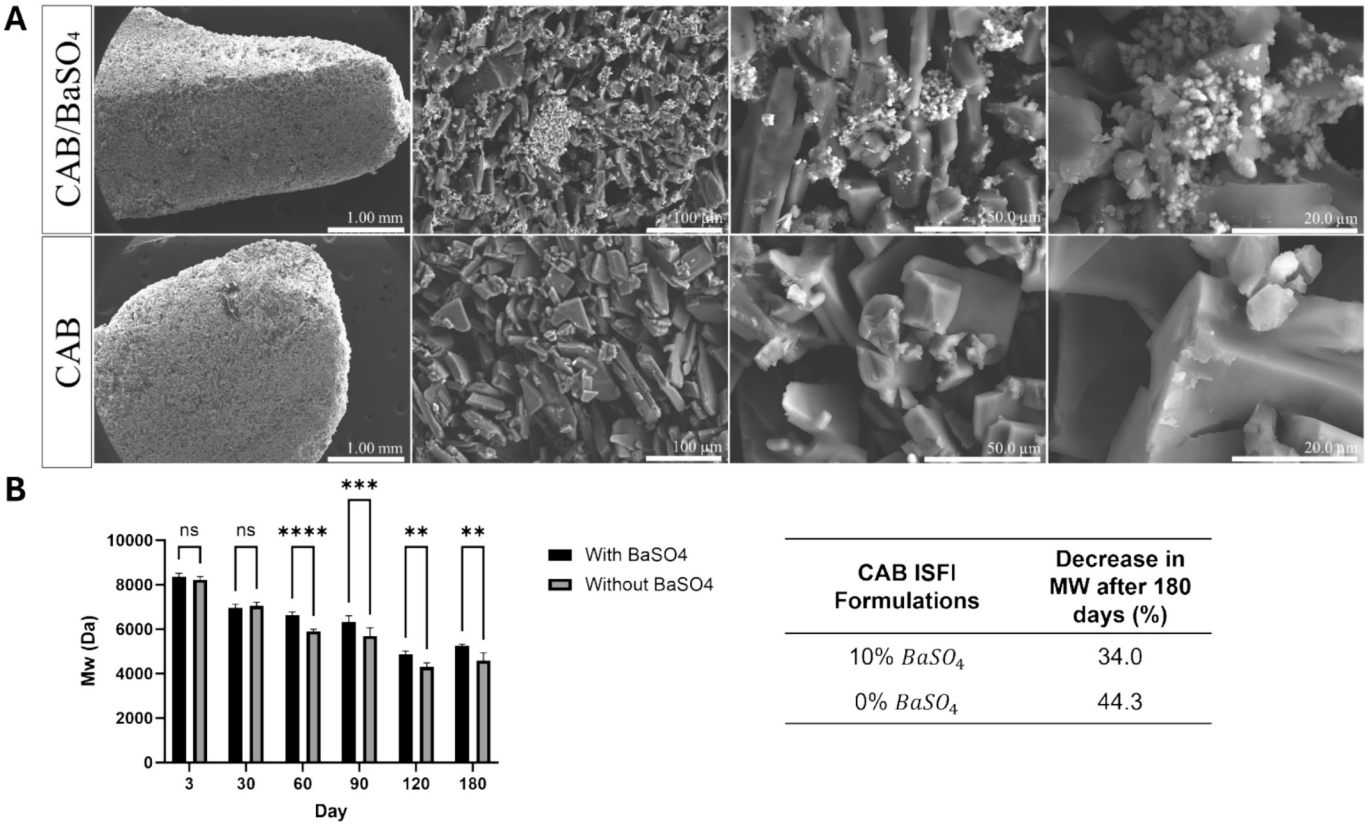

CAB ISFI Formulations	Decrease in MW after 180 days (%)
10% $BaSO_4$	34.0
0% $BaSO_4$	44.3

Fig. 2. ISFI microstructure and PLGA degradation in vitro of CAB/$BaSO_4$ and CAB ISFIs. A) ISFI microstructure of CAB/$BaSO_4$ and CAB ISFIs. SEM images of CAB/$BaSO_4$ and CAB ISFIs collected after 180 days of incubation in phosphate buffer saline (PBS, pH 7.4 with 2 % solutol) at 37 °C. Images from left to right represent increasing magnification (30×, 300×, 1000×, 2500×). Scale bars represent 1.00 mm, 100 µm, 50 µm, and 20-µm respective to increasing magnification. B) PLGA MW change in CAB/$BaSO_4$ and CAB ISFIs over time. GPC analysis of CAB/$BaSO_4$ and CAB ISFIs collected after 3, 30, 60, 90, 120, and 180 days post incubation in PBS at 37 °C. Statistical analysis: two-way ANOVA with Tukey's multiple comparisons comparing PLGA MW with respect to formulation and timepoint (ns = no significance; $^{**}p < 0.0021$; $^{***}p < 0.0002$; $^{****}p < 0.0001$).

visible differences in the physical appearance of the formulation (colour, phase separation, viscosity). On the other hand, the formulation stored at 40 °C/75 % RH for 90 days became too viscous and non-syringeable and hence, was not further investigated. After 30 days of storage, there was no significant difference in the in vitro release ($p \geq 0.9998$) between all formulations when compared to the baseline formulation (Fig. 3A). Other than the formulation stored at 40 °C/75 % RH for 90 days, all CAB/$BaSO_4$ ISFI formulations maintained sustained drug release over 30 days, achieving target release rates of approximately 40 μg/day, consistent with the in vitro release profile observed for the CAB ISFI [23]. This was also confirmed by GPC analysis quantifying depot degradation with no significant difference ($p \geq 0.4468$) observed in PLGA degradation (Fig. 3B).

While in vitro release was not significantly altered under the two storage conditions, PLGA degradation can occur upon long-term storage under those conditions. GPC analysis of the CAB/$BaSO_4$ ISFI formulation showed 0.12 % decrease in PLGA MW when stored at 4 °C and 56.27 % decrease in MW when stored under accelerated stability conditions (40 °C/75 % RH) for more than one year (Fig. 3C). Additionally, the pH of the formulation was measured before and after storage. At baseline, the pH of the formulation was neutral (pH: 6–7), with the pH becoming more acidic after one year of storage at 4 °C (pH: 5–6), and 40 °C/75 % RH (pH: 2–3). This further confirms the PLGA degradation to its lactic acid and glycolic acid byproducts. Overall, the formulation was most stable when stored at 4 °C, as demonstrated by minimum PLGA degradation (0.12 %) after 1 year and its ability to remain syringeable and injectable after 90 days storage at 4 °C with no significant change in CAB release kinetics in vitro.

3.4. In vivo safety studies in BALB/c mice

An extended (180 days) in vivo safety study was conducted in female BALB/c mice to assess the local and systemic inflammation following the injection of CAB and CAB/$BaSO_4$ ISFIs, compared to control mice that did not receive any injection. Microscopic evaluation of injection site tissues excised at multiple timepoints post ISFI administration showed that both the CAB and CAB/$BaSO_4$ ISFIs elicited minimal (early time points) to moderate (late time points) local inflammation (Fig. 4A, 4B). At early timepoints, inflammation was generally minimal and comprised primarily by low numbers of macrophages and neutrophils (Fig. 4A). The median local inflammation score increased over time (Fig. 4B), reflecting the progressive infiltration of the implant material by inflammatory cells. While both formulations exhibited similar initial inflammation levels, the CAB/$BaSO_4$ ISFI displayed distinctive histological features. Notably, the implants contained grey-tan pigment identified as $BaSO_4$, interspersed among the drug crystals. This grey-tan pigment was also observed within and external to macrophages around the implants, suggesting accumulation of the $BaSO_4$ ISFI and the inability of macrophages to clear this material. Additionally, multinucleated giant cells and cholesterol clefts, commonly associated with granulomatous inflammation, were visible in the surrounding tissues, further differentiating the inflammatory response. The presence of $BaSO_4$ appeared to alter the immune response, leading to a more granulomatous reaction with fewer neutrophils compared to the standard CAB ISFI.

Systemic inflammation was assessed by enzyme-linked immunosorbent assay (ELISA) to quantify IL-6 and TNF-α proinflammatory cytokines in plasma. Results showed no systemic acute or chronic

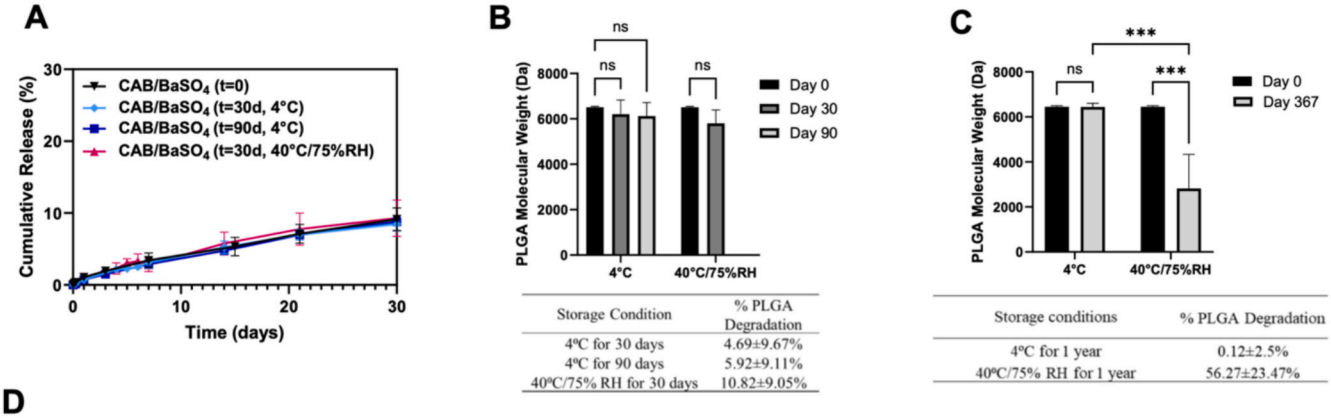

Storage Condition	% PLGA Degradation
4ºC for 30 days	4.69±9.67%
4ºC for 90 days	5.92±9.11%
40ºC/75% RH for 30 days	10.82±9.05%

Storage conditions	% PLGA Degradation
4ºC for 1 year	0.12±2.5%
40ºC/75% RH for 1 year	56.27±23.47%

D

CAB/$BaSO_4$ ISFI (500 mg/mL CAB, 10% $BaSO_4$)	CAB Concentration (mg/mL)	Depot size (mg)	CAB Burst at 24h (%)	CAB Burst at 24h (μg)	CAB Cumulative % Released at 30 days	CAB Cumulative μg Released at day 30	Release Rate (μg/day)
Baseline (0d)	491.59.±12.33	30.7±8.6	1.07±0.33	142.30±30.52	9.13±1.59	1226.33±187.42	41.98 (R^2=0.96)
30 days in 4ºC	557.02±17.76	33.7±3.7	0.75±0.13	98.53±19.6	8.46±0.96	1115.73±150.07	40.54 (R^2=0.95)
30 days in 40ºC/75%RH	550.76±28.20	30.1±6.9	0.84±0.14	108.17±28.03	9.29±2.52	1159.10±124.68	42.11 (R^2=0.95)
90 days in 4ºC	434.00±14.43	29.1±4.2	0.71±0.02	80.30±6.95	8.79±0.57	994.21±41.22	35.53 (R^2=0.99)

Fig. 3. CAB/$BaSO_4$ ISFI stability and post-storage in vitro release kinetics. A) Cumulative in vitro release kinetics of CAB/$BaSO_4$ ISFI (500 mg/mL CAB (1:4 w/w PLGA:solvent) with 10 wt% $BaSO_4$) at baseline ($t = 0$), 30 days, and 90 days post storage at 4 °C and 40 °C/75 % RH. All in vitro release studies were done in phosphate buffer saline (PBS, pH 7.4 with 2 % solutol) at 37 °C under sink conditions. Data presented as an average ± standard deviation for $n = 4$ samples. Statistical analysis: two-way ANOVA with Tukey's multiple comparisons comparing CAB release with respect to formulation and timepoint. By day 30 post-storage in vitro release, all storage formulations except for the formulation stored for 90 days in accelerated conditions, showed no significant CAB release compared to the baseline ($p > 0.05$). B) Effect of storage conditions on PLGA MW post 30-day in vitro release determined by gel permeation chromatography (GPC) analysis. Statistical analysis: two-way ANOVA with Tukey's multiple comparisons comparing PLGA MW with respect to time in storage and storage condition (ns = no significance). C) Effect of long-term (> 1 year) storage at 4 °C and 40 °C/75 % RH on PLGA MW determined by GPC analysis. Statistical analysis: two-way ANOVA with Tukey's multiple comparisons comparing PLGA MW with respect to time in storage and storage condition (ns = no significance; ***$p < 0.0002$). D) Summary table of CAB/$BaSO_4$ ISFI post storage in vitro release kinetics.

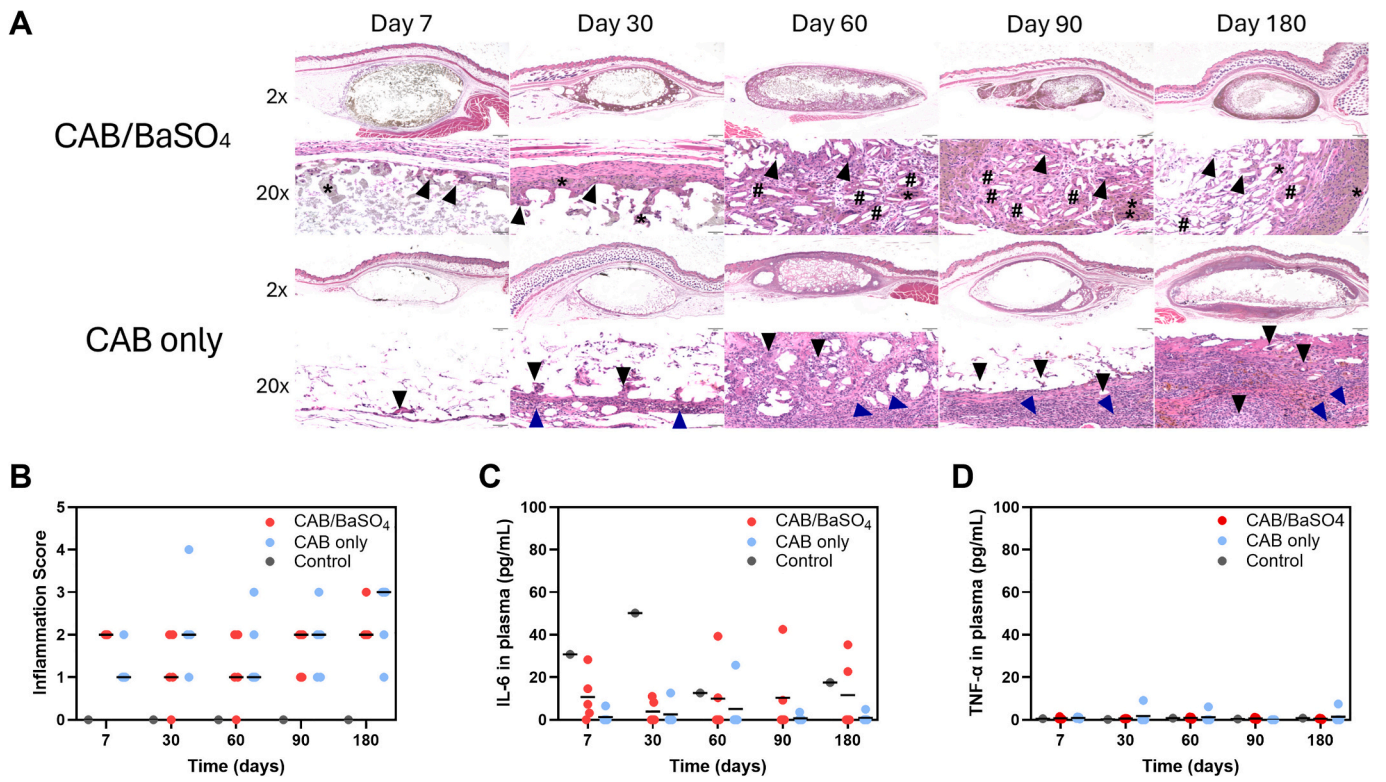

Fig. 4. In vivo safety evaluation of CAB/$BaSO_4$ ISFIs in BALB/c mice. A) Local inflammation of excised depots and surrounding subcutaneous tissue collected at day 7, 30, 60, 90, and 180 post ISFI administration (n = 4–5/timepoint for CAB/$BaSO_4$ and CAB ISFI treated mice and n = 1/timepoint for control (no injection) mice) and stained with H&E. Arrows indicate infiltrated immune cells and areas of inflammation (black arrows indicate macrophages, blue arrows indicate neutrophils). Asterisks (*) denote pigmented macrophages. Pound signs (#) identifies cholesterol clefts. Additional pictures and scores are shown in Supplementary Fig. 8 and 9. B) Inflammatory scores of subcutaneous tissue surrounding the depot evaluated using a light microscope and scored blindly by a board-certified pathologist. Black bars represent the median inflammatory score at each timepoint (n = 5 per timepoint). C) Concentration of IL-6 (pg/mL) in plasma quantified by ELISA at day 7, 30, 60, 90, and 180 post ISFI administration (n = 5/timepoint for CAB/$BaSO_4$ and CAB ISFI treated mice and n = 1/timepoint for control (no injection) mice). Black bars represent the mean concentration of IL-6 at each timepoint. D) Concentration of TNF-α (pg/mL) in plasma quantified by ELISA at day 7, 30, 60, 90, 180 post ISFI administration (n = 5/timepoint for CAB/$BaSO_4$ and CAB ISFI treated mice and n = 1/timepoint for control (no injection) mice). Black bars represent the mean concentration of TNF-α at each timepoint. (For interpretation of the references to colour in this figure legend, the reader is referred to the web version of this article.)

inflammation. IL-6 levels ranged between 0 and 26 pg/mL for CAB ISFI (p = 0.004) and 0–43 pg/mL for CAB/$BaSO_4$ ISFI (p = 0.0119) with mean levels significantly less than the no-injection control group (Fig. 4C). TNF-α levels ranged between 0 and 2 pg/mL for CAB ISFI (p = 0.8496) and 0–9 pg/mL for CAB/$BaSO_4$ ISFI (p = 0.9924) with mean levels comparable to the control group (Fig. 4D). Overall, the results demonstrate that the CAB and CAB/$BaSO_4$ ISFIs were well tolerated and considered safe, with no overt signs of toxicity or chronic inflammation.

3.5. *In vivo pharmacokinetics and assessment of pharmacokinetics tail and biodistribution of CAB in CAB/$BaSO_4$ ISFI*

Pharmacokinetics studies were conducted in female BALB/c mice to investigate time to completion (TTC) PK and PK tail post depot removal. The average CAB plasma concentration was 60-fold greater than the 4 × PA-IC_{90} (664 ng/mL) benchmark for HIV pre-exposure prophylaxis (PrEP) (Fig. 5A). Moreover, there was no significant difference in plasma CAB concentrations between the CAB and CAB/$BaSO_4$ ISFIs (p = 0.9671) for up to 330 days. CAB plasma concentration was sustained above the 4 × IC_{90} benchmark for up to 390 days with the CAB/$BaSO_4$ ISFI, which was slightly longer compared to the original CAB ISFI (<360 days). The in vivo release data corroborates the in vitro results demonstrating a slower PLGA degradation and slower release kinetics in the presence of $BaSO_4$, thereby achieving longer sustained release in vivo with the CAB/$BaSO_4$ ISFI.

To further assess the PK tail, CAB/$BaSO_4$ ISFI was administered to female BALB/c mice, and depots were removed 180 days post ISFI administration. Plasma samples were collected longitudinally for up to 60 days post depot removal to assess the PK tail (Fig. 5B). Within 7 days post depot removal, CAB plasma concentrations reached below the 1× PA-IC_{90} (166 ng/mL) in 5 out of 6 mice. At day 14 post depot removal, CAB plasma concentrations reached LLOQ (25 ng/mL) in 5 out of 6 mice. At day 30 post depot removal, all mice elicited plasma concentrations below the 1× PA-IC_{90} limit (Fig. 5B). The presence of a CAB plasma PK tail after depot removal was previously hypothesized to result from the high dose of CAB administered to mice (1215 mg/kg), which leads to drug accumulation in the injection site subcutaneous tissue surrounding the depot [24]. To investigate this hypothesis, we performed a comprehensive biodistribution study where CAB ISFI or CAB/$BaSO_4$ ISFI were administered to female BALB/c mice and at day 180 post ISFI administration, mice were euthanized and various tissues and organs – including cervix, rectum, vagina, cervical lymph nodes (LN), axillary LN, inguinal LN, duodenum, ileum, colon, liver, spleen, subcutaneous tissue and plasma – were collected and analyzed for CAB concentration using high-performance liquid chromatography-tandem mass spectrometry (LC/MS-MS) analysis. In the CAB ISFI group, CAB concentration in plasma and tissues remained relatively stable over time, while concentrations in the subcutaneous tissue declined significantly, particularly between day 60 and day 180 (p < 0.0001; Supplementary Fig. 12), consistent with depot erosion. At day 180, both CAB ISFI and CAB/$BaSO_4$ ISFI groups had the highest CAB concentrations detected in the subcutaneous tissue, with lower concentrations observed across the other tissues (Fig. 5C). Notably, the CAB/$BaSO_4$ ISFI group had less variability across most tissues compared to the CAB ISFI group, with

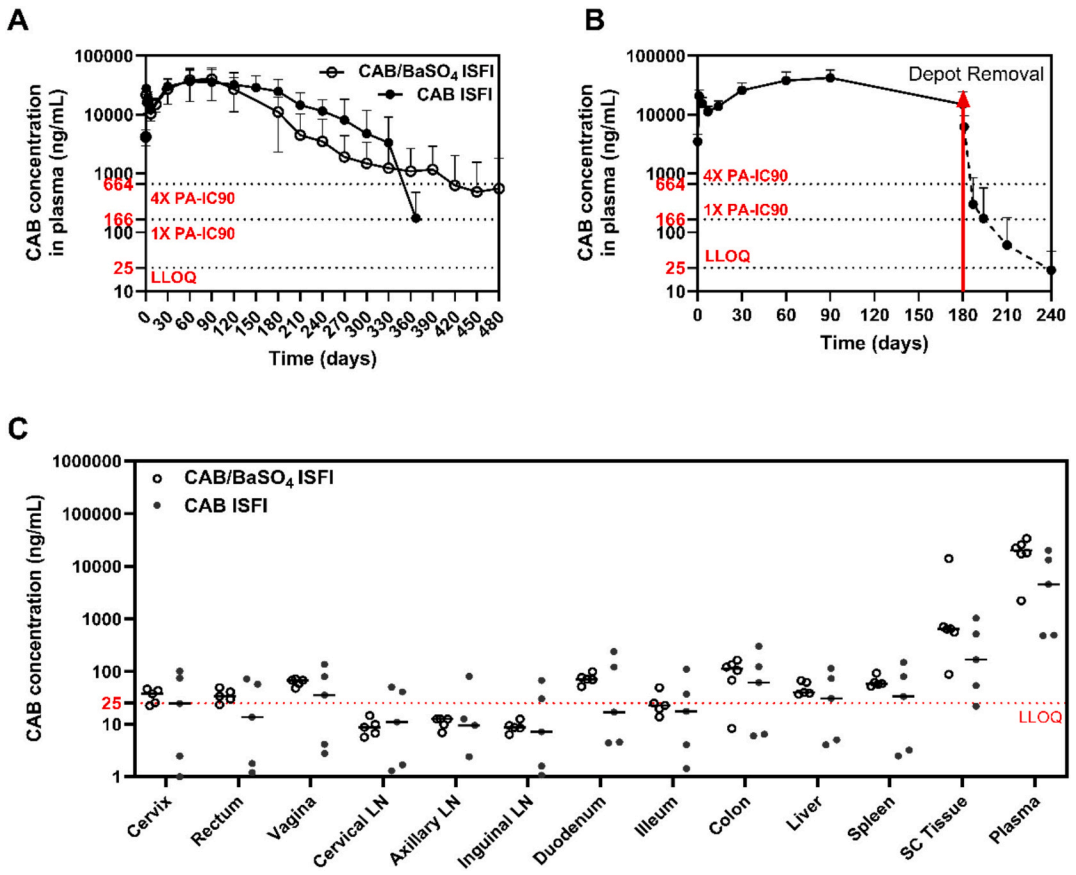

Fig. 5. In vivo pharmacokinetics and biodistribution studies in BALB/c mice. A) In vivo pharmacokinetic (PK) profile of CAB/$BaSO_4$ ISFI compared to CAB ISFI. CAB concentration (average ± standard deviation) in plasma for up to 480 days ($n = 6$ per timepoint). 1× and 4× PA-IC90 values are indicated with dotted lines for CAB (166 ng/mL and 664 ng/mL respectively). Plasma concentrations of individual mice are illustrated in Supplementary Fig. 10. B) In vivo evaluation of PK tail of CAB/$BaSO_4$ ISFIs in BALB/c mice. Implants were removed 180 days post ISFI administration. CAB concentration (average ± standard deviation) in plasma was determined up to 60 days post-implant removal (n = 6 per timepoint). 1× and 4× PA-IC90 values are indicated with dotted lines for CAB (166 ng/mL and 664 ng/mL respectively). Plasma concentrations of individual mice are illustrated in Supplementary Fig. 11. C) Biodistribution of CAB across multiple organs, injection site subcutaneous tissue, and plasma. CAB concentrations in organs from mice administered with CAB ISFI are shown in Supplementary Fig. 12. CAB biodistribution for mice administered with the standard CAB/$BaSO_4$ ISFI formulation are shown in Supplementary Fig. 13.

lower coefficient of variation (%CV) values except for the subcutaneous tissue (Supplementary Fig. 14). This may reflect the denser nature of the CAB/$BaSO_4$ ISFI formulation, which results in slower drug release and more retention at the injection site. Along with the prior findings on depot removal shortening the plasma tail, this suggests that the distal tissues do not function as long-term reservoirs, and that the subcutaneous depot is the primary route of sustained systemic exposure.

3.6. In vivo CAB/$BaSO_4$ ISFI residual drug quantification and biodegradation

The CAB/$BaSO_4$ ISFIs were successfully retrieved from mice after 180 days via a small skin incision at the injection site, which notably showed no surrounding fibrotic tissue around the depot (Fig. 6A). This minimal fibrosis is indicative of good biocompatibility of the implant material, suggesting that the addition of $BaSO_4$ does not provoke excessive fibrotic reactions. The excised depots were analyzed to assess in vivo degradation and quantify the residual drug content. CAB/$BaSO_4$ ISFIs excised at day 180 post administration exhibited approximately 68 % mass loss, and 82.2 % PLGA degradation, with about 26.6 % of the original CAB dose remaining within the depots. These results confirm the ability of the CAB/$BaSO_4$ ISFI depots to remain intact during retrieval, and that the depots can potentially sustain CAB release beyond 180 days.

4. Discussion

The development of ultra-long-acting, removable ISFIs represents a significant advancement in the field of HIV PrEP. These technologies address key challenges associated with currently available preventative options, primarily related to patient adherence and potential drug resistance. Building on our prior work with the ultra-long-acting CAB ISFI, the development of the CAB/$BaSO_4$ ISFI makes the ISFI radiopaque, thus enabling non-invasive in vivo visualization using full-body X-ray imaging to facilitate potential depot removal and investigate potential depot migration over time. This formulation advances HIV-PrEP by combining extended protection against HIV with less frequent dosing requirements with the option, not the requirement, of being removable. In typical cases, most users would benefit from the six-month injection without any further intervention, maintaining low-cost, compliance, and accessibility. The additional $BaSO_4$ simply adds the ability to locate the depot non-invasively using X-ray imaging in scenarios requiring treatment discontinuation due to side effects, adverse injection site reactions, or when transitioning between different therapies. The ability to visually confirm implant integrity and location via X-ray imaging is attributed to the inclusion of a contrast agent, $BaSO_4$, in the ISFI further aligning with the goals of personalized medicine, offering tailored treatment plans with improved patient compliance. Throughout the study, there was no significant evidence of implant migration, indicating that the CAB/$BaSO_4$ ISFI remained at the injection site, reducing

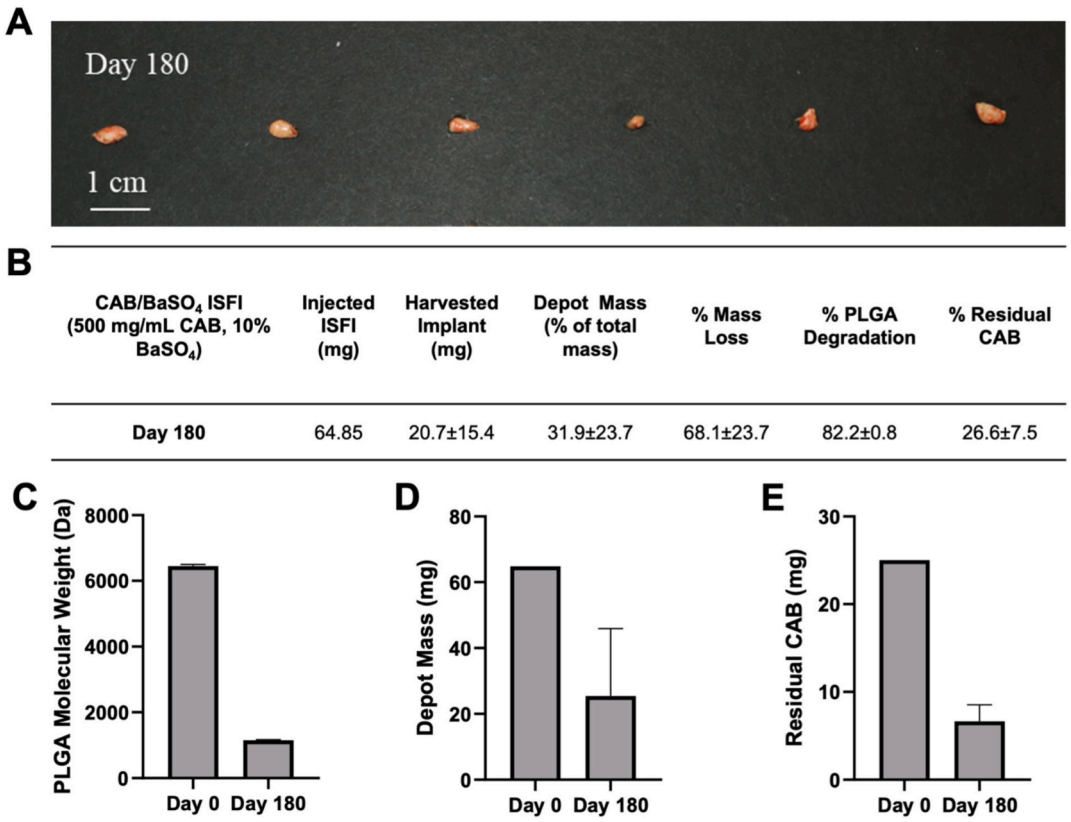

CAB/$BaSO_4$ ISFI (500 mg/mL CAB, 10% $BaSO_4$)	Injected ISFI (mg)	Harvested Implant (mg)	Depot Mass (% of total mass)	% Mass Loss	% PLGA Degradation	% Residual CAB
Day 180	64.85	20.7±15.4	31.9±23.7	68.1±23.7	82.2±0.8	26.6±7.5

Fig. 6. Depot degradation and residual drug after 180 days of in vivo release. A) Image of CAB/$BaSO_4$ depots retrieved from mice 180 days post ISFI administration. B) Table summary of changes in depot mass, PLGA MW, and residual drug relative to time zero. C) Average CAB/$BaSO_4$ depot mass at day 180 post ISFI administration to mice ($n = 6$). Day 0 masses were calculated based on a 50 μL injection volume and using the density of the formulation (1.297 g/mL) to determine approximate depot mass injected into release media. D) PLGA MW (weight average MW) of CAB/$BaSO_4$ ISFI 180 days post ISFI administration to mice ($n = 3$). Day 0 PLGA MW was based on neat PLGA (10 kDa). E) Residual CAB in CAB/$BaSO_4$ depots at day 180 post ISFI administration to mice (n = 3) compared to the initial dose at day 0 (~25 mg).

potential complications associated with implant displacement. Of note, based on the present results from the X-imaging studies in mice and in macaques (separate publication), demonstrating lack of depot migration over several months, the use of $BaSO_4$ will likely not be required for clinical translation of these formulations, and the absence of $BaSO_4$ will reduce formulation complexity and cost.

The combined findings from in vitro release studies, depot degradation, and SEM/SEM-EDX imaging provide a comprehensive understanding of the slower in vitro release rates of CAB observed with CAB/$BaSO_4$ ISFIs compared to the original CAB ISFI formulation. The in vitro release studies demonstrated that the presence of $BaSO_4$ extended the release duration of CAB as a result of a denser and more compact microstructure of the resulting depot. This impact was demonstrated by the higher density (1.297 g/mL) of the CAB/$BaSO_4$ ISFI and SEM/SEM-EDX analyses of the internal microstructure, where $BaSO_4$ particles were densely dispersed between the CAB crystals within the polymer matrix. This dense microstructure can lead to reduced diffusion pathways for water inflex and the drug, thereby slowing PLGA degradation via hydrolysis and drug release via both diffusion and polymer degradation. SEM-EDX analysis confirmed the presence and distribution of $BaSO_4$ within the CAB/$BaSO_4$ ISFI, validating the components within the polymer matrix. PLGA degradation was quantified using GPC analysis, and results showed no significant differences in PLGA MW between the CAB ISFI and the CAB/$BaSO_4$ ISFI formulations at day 30 of in vitro release. However, at day 180, the CAB/$BaSO_4$ ISFI exhibited a 34 % decrease in PLGA MW compared to a 44.3 % decrease for the CAB ISFI, further supporting the slower depot degradation in the presence of $BaSO_4$. Additionally, the PK profile of the CAB/$BaSO_4$ ISFI demonstrates its ability to maintain therapeutic concentrations of CAB in plasma for more than 390 days. Plasma concentrations reached up to 40.36–117.02 folds higher than the 4 × PA-IC90 benchmark, remaining above this threshold for 390 days, which is significantly higher than previously reported long-acting CAB formulations [38–40].

The CAB/$BaSO_4$ ISFI formulation was syringeable using a 19G needle for subcutaneous administration in mice and was safe and well-tolerated without any severe injection site reactions or systemic inflammation. Depots were successfully removed via a small skin incision at day 180 post ISFI administration and elicited minimal fibrotic tissue formation around the depot. Histological analysis showed minimal to moderate local inflammation, characterized by infiltrated immune cells around the depot, which diminished over time. Notably, results showed no significant systemic inflammation, as indicated by stable levels of IL-6 and TNF-α pro-inflammatory cytokines. Additionally, there was no evidence of significant implant migration over 268 days, demonstrating the ability to localize the depot for potential removability. This is especially important, as the ability to remove the CAB/$BaSO_4$ ISFI if required is critical in scenarios where discontinuation of treatment is necessary, offering a safe and efficient method to cease drug delivery without invasive procedures. Furthermore, the CAB/$BaSO_4$ ISFI elicited a short PK tail post depot removal at day 180 with CAB concentrations reaching LLOQ within 30 days post depot removal. This short PK tail minimizes prolonged drug exposure, thereby reducing the potential for a drug-resistant virus. Overall, these results demonstrate that the radiopaque CAB/$BaSO_4$ ISFI was well-tolerated in mice for long-term use, and depots can be removed if needed, providing a reliable and effective option for HIV PrEP with minimal adverse effects. Ultimately, future studies include advancing a once- or twice-yearly CAB ISFI to macaques due to their high clinical relevance. These studies include (1)

administering 2× 1 mL subcutaneous injections of CAB ISFI to macaques to assess PK, safety, efficacy, and PK after re-dose to establish a dosing schedule, (2) time to completion PK and PK tail studies, (3) establishing processes for Good Manufacturing Practice (GMP), Chemistry, Manufacturing, and Controls (CMC), and initiating Investigational New Drug (IND)-enabling studies. We anticipate a similar injection volume (2× 1 mL SC injections) when translating to humans, if non-human primate studies are successful.

5. Conclusion

We demonstrate the ability to formulate an injectable, biodegradable CAB/$BaSO_4$ ISFI that successfully combines the benefits of sustained release, radiopacity, and removability, making it a highly promising option for HIV PrEP. The addition of $BaSO_4$ enhances implant visualization and contributes to a controlled release mechanism, ensuring consistent medication delivery and potentially improving adherence and treatment outcomes. The CAB/$BaSO_4$ ISFI elicited sustained release in vitro at target in vitro release rates (≥40 μg/day) post 30 days of storage under accelerated stability conditions (40 °C/75 % RH). Furthermore, the formulation elicited sustained release over 390 days in vivo, with CAB plasma concentrations reaching well above the established PK benchmark for protection (≥4 × PA-IC_{90}). The CAB/$BaSO_4$ ISFI elicited a short PK tail post depot removal with CAB plasma concentration reaching BLOQ within 30 days post removal. The CAB/$BaSO_4$ ISFIs were safe and well-tolerated with no severe injection site reactions or systemic inflammation for up to 180 days. This study demonstrates promising in vitro and in vivo results that highlight the ability of radiopaque CAB ISFI to expand the preventative options available for PrEP around the world.

CRediT authorship contribution statement

Thy Le: Writing – review & editing, Writing – original draft, Visualization, Methodology, Investigation, Formal analysis, Data curation. **Isabella C. Young:** Formal analysis, Data curation. **Jasmine L. King:** Writing – review & editing. **Mackenzie L. Cottrell:** Writing – review & editing, Writing – original draft, Supervision, Funding acquisition, Formal analysis, Data curation. **Amar Shankar Kumbhar:** Formal analysis, Data curation. **Craig Sykes:** Writing – review & editing, Writing – original draft, Formal analysis, Data curation. **Amanda Schauer:** Writing – original draft. **Gabriela De la Cruz:** Data curation. **Caleb T. Kozuszek:** Data curation. **Nanditha Chundayil Kalathil:** Data curation. **Alexandra Abel:** Data curation. **Rani S. Sellers:** Writing – review & editing, Writing – original draft, Software, Formal analysis. **Angela D.M. Kashuba:** Supervision, Resources, Funding acquisition. **S. Rahima Benhabbour:** Writing – review & editing, Writing – original draft, Supervision, Software, Resources, Project administration, Methodology, Funding acquisition, Conceptualization.

Funding

This work was supported by the National Institute of Allergy and Infectious Diseases (grant numbers R01AI162246 and R01AI176949 to SRB). The content is solely the responsibility of the authors and does not necessarily represent the official views of the National Institute of Allergy and Infectious Diseases. Any opinion, findings, and conclusions, or recommendations expressed in this material are those of the authors(s) and do not necessarily reflect the views of the National Science Foundation. This research was supported by the University of North Carolina at Chapel Hill Center For AIDS Research (CFAR), an NIH funded program P30AI05410.

Declaration of competing interest

SRB and ICY are inventors on a patent describing the Injectable Polymer Based Drug Formulation for Ultra-Long-Acting Drug Delivery.

Acknowledgements

We would like to thank the UNC Preclinical Research Unit (PRU) for assisting with the mouse CAB/$BaSO_4$ ISFI injections and sample collections, the UNC Clinical Pharmacology and Analytical Chemistry Core (CPAC), particularly Lauren Tompkins, and Chapel Hill Analytical and Microscopy Services Laboratory.

Appendix A. Supplementary data

Supplementary data to this article can be found online at https://doi.org/10.1016/j.jconrel.2025.114166.

Data availability

Data will be made available on request.

References

[1] D. Sidebottom, A.M. Ekström, S. Strömdahl, A systematic review of adherence to oral pre-exposure prophylaxis for HIV – How can we improve uptake and adherence? BMC Infect. Dis. 18 (2018) 581, https://doi.org/10.1186/s12879-018-3463-4.

[2] S.K. Calabrese, K. Underhill, How stigma surrounding the use of HIV preexposure prophylaxis undermines prevention and pleasure: a call to destigmatize "Truvada Whores,", Am. J. Public Health 105 (2015) 1960–1964, https://doi.org/10.2105/ajph.2015.302816.

[3] R.J. Landovitz, D. Donnell, M.E. Clement, B. Hanscom, L. Cottle, L. Coelho, R. Cabello, S. Chariyalertsak, E.F. Dunne, I. Frank, J.A. Gallardo-Cartagena, A. H. Gaur, P. Gonzales, H.V. Tran, J.C. Hinojosa, E.G. Kallas, C.F. Kelley, M.H. Losso, J.V. Madruga, K. Middelkoop, N. Phanuphak, B. Santos, O. Sued, J.V. Huamaní, E. T. Overton, S. Swaminathan, C.D. Rio, R.M. Gulick, P. Richardson, P. Sullivan, E. Piwowar-Manning, M. Marzinke, C. Hendrix, M. Li, Z. Wang, J. Marrazzo, E. Daar, A. Asmelash, T.T. Brown, P. Anderson, S.H. Eshleman, M. Bryan, C. Blanchette, J. Lucas, C. Psaros, S. Safren, J. Sugarman, H. Scott, J.J. Eron, S. D. Fields, N.D. Sista, K. Gomez-Feliciano, A. Jennings, R.M. Kofron, T.H. Holtz, K. Shin, J.F. Rooney, K.Y. Smith, W. Spreen, D. Margolis, A. Rinehart, A. Adeyeye, M.S. Cohen, M. McCauley, B. Grinsztejn, H. 083 S. Team, Cabotegravir for HIV prevention in cisgender men and transgender women, N. Engl. J. Med. 385 (2021) 595–608, https://doi.org/10.1056/nejmoa2101016.

[4] S. Delany-Moretlwe, J.P. Hughes, P. Bock, S.G. Ouma, P. Hunidzarira, D. Kalonji, N. Kayange, J. Makhema, P. Mandima, C. Mathew, E. Spooner, J. Mpendo, P. Mukwekwerere, N. Mgodi, P.N. Ntege, G. Nair, C. Nakabiito, H. Nuwagaba-Biribonwoha, R. Panchia, N. Singh, B. Siziba, J. Farrior, S. Rose, P.L. Anderson, S. H. Eshleman, M.A. Marzinke, C.W. Hendrix, S. Beigel-Orme, S. Hosek, E. Tolley, N. Sista, A. Adeyeye, J.F. Rooney, A. Rinehart, W.R. Spreen, K. Smith, B. Hanscom, M.S. Cohen, M.C. Hosseinipour, H. 084 Study Group, A. Asmelash, A. Sehurutshi, A. Baguma, A. Marais, B. Kawoozo, B.P. Malinga, B.G. Mirembe, B. Okech, B. Esterhuizen, C. Murombedzi, D. Gadama, E. Hwengwere, E. Roos, E.S. Magada, E. Shava, E. Piwowar-Manning, E. Tahuringana, F.G. Muhlanga, F. Conradie, F. Angira, G. Nanyonjo, G. Kistnasami, H. Mvula, I. Naidoo, J. Horak, J. Jere, J. Moodley, K. Shin, K. Nel, K. Bokoch, L. Birungi, L. Emel, M. Monametsi, M. Sibanda, M. Mutambanengwe, M. Chitukuta, M. Matimbira, M. Bhondai-Mhuri, N. Sibisi, N. Morar, N. Mudzonga, P. Natureeba, P. Richardson, P. Musara, P. Macdonald, R. Nkambule, R. Mosime, R. White, R. Berhanu, R. Ncube-Sihlongonyane, R. Sekabira, S. Siva, S. Pillay, S. Govender, S. Bamweyana, S. Nzimande, S. Innes, S. Dadabhai, T. Samandari, T. Tembo, T.L. Mabedi, T. Chirenda, T. Chidemo, V. Mudhune, V. Naidoo, W. Samaneka, Y. Agyei, Y. Musodza, Y. Fourie, Z. Gaffoor, Cabotegravir for the prevention of HIV-1 in women: results from HPTN 084, a phase 3, randomised clinical trial, Lancet 399 (2022) 1779–1789, https://doi.org/10.1016/s0140-6736(22)00538-4.

[5] R.J. Landovitz, B.S. Hanscom, M.E. Clement, H.V. Tran, E.G. Kallas, M. Magnus, O. Sued, J. Sanchez, H. Scott, J.J. Eron, C. del Rio, S.D. Fields, M.A. Marzinke, S. H. Eshleman, D. Donnell, M.A. Spinelli, R.M. Kofron, R. Berman, E.M. Piwowar-Manning, P.A. Richardson, P.A. Sullivan, J.P. Lucas, P.L. Anderson, C.W. Hendrix, A. Adeyeye, J.F. Rooney, A.R. Rinehart, M.S. Cohen, M. McCauley, B. Grinsztejn, H. 083 S. Team, Efficacy and safety of long-acting cabotegravir compared with daily oral tenofovir disoproxil fumarate plus emtricitabine to prevent HIV infection in cisgender men and transgender women who have sex with men 1 year after study unblinding: a secondary analysis of the phase 2b and 3 HPTN 083 randomised controlled trial, Lancet HIV 10 (2023) e767–e778, https://doi.org/10.1016/s2352-3018(23)00261-8.

[6] R.J. Landovitz, S. Li, J.J. Eron, B. Grinsztejn, H. Dawood, A.Y. Liu, M. Magnus, M. C. Hosseinipour, R. Panchia, L. Cottle, G. Chau, P. Richardson, M.A. Marzinke, S. H. Eshleman, R. Kofron, A. Adeyeye, D. Burns, A.R. Rinehart, D. Margolis, M. S. Cohen, M. McCauley, C.W. Hendrix, Tail-phase safety, tolerability, and pharmacokinetics of long-acting injectable cabotegravir in HIV-uninfected adults: a

secondary analysis of the HPTN 077 trial, Lancet HIV 7 (2020) e472–e481, https://doi.org/10.1016/s2352-3018(20)30106-5.
[7] UNAIDS, Global HIV & AIDS Statistics - Fact Sheet 2024. https://www.unaids.org/en/resources/fact-sheet, 2024.
[8] UNAIDS, 2024 Global AIDS Report — The Urgency of Now: AIDS at a Crossroads. https://www.unaids.org/sites/default/files/media_asset/2024-unaids-global-aids-update_en.pdf, 2024.
[9] R.C. Gallo, L. Montagnier, The discovery of HIV as the cause of AIDS, N. Engl. J. Med. 349 (2003) 2283–2285, https://doi.org/10.1056/nejmp038194.
[10] S.S.A. Karim, Q.A. Karim, Antiretroviral prophylaxis: a defining moment in HIV control, Lancet 378 (2012) e23–e25, https://doi.org/10.1016/s0140-6736(11)61136-7.
[11] R.M. Granich, C.F. Gilks, C. Dye, K.M.D. Cock, B.G. Williams, Universal voluntary HIV testing with immediate antiretroviral therapy as a strategy for elimination of HIV transmission: a mathematical model, Lancet 373 (2009) 48–57, https://doi.org/10.1016/s0140-6736(08)61697-9.
[12] S. Dixon, S. McDonald, J. Roberts, The impact of HIV and AIDS on Africa's economic development, BMJ 324 (2002) 232, https://doi.org/10.1136/bmj.324.7331.232.
[13] M.S. Cohen, Y.Q. Chen, M. McCauley, T. Gamble, M.C. Hosseinipour, N. Kumarasamy, J.G. Hakim, J. Kumwenda, B. Grinsztejn, J.H.S. Pilotto, S. V. Godbole, S. Mehendale, S. Chariyalertsak, B.R. Santos, K.H. Mayer, I.F. Hoffman, S.H. Eshleman, E. Piwowar-Manning, L. Wang, J. Makhema, L.A. Mills, G. de Bruyn, I. Sanne, J. Eron, J. Gallant, D. Havlir, S. Swindells, H. Ribaudo, V. Elharrar, D. Burns, T.E. Taha, K. Nielsen-Saines, D. Celentano, M. Essex, T.R. Fleming, H. 052 S. Team, Prevention of HIV-1 infection with early antiretroviral therapy, N. Engl. J. Med. 365 (2011) 493–505, https://doi.org/10.1056/nejmoa1105243.
[14] J.A. Catania, S.M. Kegeles, T.J. Coates, Towards an understanding of risk behavior: an AIDS risk reduction model (ARRM), Health Educ. Behav. 17 (1990) 53–72, https://doi.org/10.1177/109019819001700107.
[15] T.J. Coates, L. Richter, C. Caceres, Behavioural strategies to reduce HIV transmission: how to make them work better, Lancet 372 (2008) 669–684, https://doi.org/10.1016/s0140-6736(08)60886-7.
[16] R.M. Grant, J.R. Lama, P.L. Anderson, V. McMahan, A.Y. Liu, L. Vargas, P. Goicochea, M. Casapía, J.V. Guanira-Carranza, M.E. Ramirez-Cardich, O. Montoya-Herrera, T. Fernández, V.G. Veloso, S.P. Buchbinder, S. Chariyalertsak, M. Schechter, L.-G. Bekker, K.H. Mayer, E.G. Kallás, K.R. Amico, K. Mulligan, L. R. Bushman, R.J. Hance, C. Ganoza, P. Defechereux, B. Postle, F. Wang, J. J. McConnell, J.-H. Zheng, J. Lee, J.F. Rooney, H.S. Jaffe, A.I. Martinez, D. N. Burns, D.V. Glidden, iPrEx S. Team, Preexposure chemoprophylaxis for HIV prevention in men who have sex with men, N. Engl. J. Med. 363 (2010) 2587–2599, https://doi.org/10.1056/nejmoa1011205.
[17] C.B. Hare, J. Coll, P. Ruane, J.-M. Molina, K.H. Mayer, H. Jessen, R.M. Grant, J.J. D. Wet, M. Thompson, E. DeJesus, R. Ebrahimi, R.M. Giler, M. Das, D. Brainard, S. McCallister, The Phase 3 Discover Study: Daily F/TAF or F/TDF for HIV Preexposure Prophylaxis. https://www.croiconference.org/abstract/phase-3-discover-study-daily-ftaf-or-ftdf-hiv-preexposure-prophylaxis/, 2025.
[18] L.V. Damme, A. Corneli, K. Ahmed, K. Agot, J. Lombaard, S. Kapiga, M. Malahleha, F. Owino, R. Manongi, J. Onyango, L. Temu, M.C. Monedi, P. Mak'Oketch, M. Makanda, I. Reblin, S.E. Makatu, L. Saylor, H. Kiernan, S. Kirkendale, C. Wong, R. Grant, A. Kashuba, K. Nanda, J. Mandala, K. Fransen, J. Deese, T. Crucitti, T. D. Mastro, D. Taylor, F.-P.S. Group, Preexposure prophylaxis for HIV infection among African women, N. Engl. J. Med. 367 (2012) 411–422, https://doi.org/10.1056/nejmoa1202614.
[19] E.O. Murchu, L. Marshall, C. Teljeur, P. Harrington, C. Hayes, P. Moran, M. Ryan, Oral pre-exposure prophylaxis (PrEP) to prevent HIV: a systematic review and meta-analysis of clinical effectiveness, safety, adherence and risk compensation in all populations, BMJ Open 12 (2022) e048478, https://doi.org/10.1136/bmjopen-2020-048478.
[20] C. Orkin, K. Arasteh, M.G. Hernández-Mora, V. Pokrovsky, E.T. Overton, P.-M. Girard, S. Oka, S. Walmsley, C. Bettacchi, C. Brinson, P. Philibert, J. Lombaard, M. St, H. Clair, S.L. Crauwels, P. Ford, V. Patel, R. Chounta, S. D'Amico, D. Vanveggel, A. Dorey, S. Cutrell, D.A. Griffith, P.E. Margolis, W. Williams, K. Y. Parys, W.R. Spreen Smith, Long-acting Cabotegravir and Rilpivirine after Oral induction for HIV-1 infection, N. Engl. J. Med. 382 (2020) 1124–1135, https://doi.org/10.1056/nejmoa1909512.
[21] E.T. Overton, G. Richmond, G. Rizzardini, H. Jaeger, C. Orrell, F. Nagimova, F. Bredeek, M.G. Deltoro, S. Swindells, J.F. Andrade-Villanueva, A. Wong, M.-A. Khuong-Josses, R.V. Solingen-Ristea, V. van Eygen, H. Crauwels, S. Ford, C. Talarico, P. Benn, Y. Wang, K.J. Hudson, V. Chounta, A. Cutrell, P. Patel, M. Shaefer, D.A. Margolis, K.Y. Smith, S. Vanveggel, W. Spreen, Long-acting cabotegravir and rilpivirine dosed every 2 months in adults with HIV-1 infection (ATLAS-2M), 48-week results: a randomised, multicentre, open-label, phase 3b, non-inferiority study, Lancet 396 (2021) 1994–2005, https://doi.org/10.1016/s0140-6736(20)32666-0.
[22] S.R. Benhabbour, M. Kovarova, C. Jones, D.J. Copeland, R. Shrivastava, M. D. Swanson, C. Sykes, P.T. Ho, M.L. Cottrell, A. Sridharan, S.M. Fix, O. Thayer, J. M. Long, D.J. Hazuda, P.A. Dayton, R.J. Mumper, A.D.M. Kashuba, J.V. Garcia, Ultra-long-acting tunable biodegradable and removable controlled release implants for drug delivery, Nat. Commun. 10 (2019) 4324, https://doi.org/10.1038/s41467-019-12141-5.
[23] I.C. Young, I. Massud, M.L. Cottrell, R. Shrivastava, P. Maturavongsadit, A. Prasher, A. Wong-Sam, C. Dinh, T. Edwards, V. Mrotz, J. Mitchell, J.N. Seixas, A. Pallerla, A. Thorson, A. Schauer, C. Sykes, G.D. la Cruz, S.A. Montgomery, A.D.M. Kashuba, W. Heneine, C.W. Dobard, M. Kovarova, J.V. Garcia, J.G. García-Lerma, S. R. Benhabbour, Ultra-long-acting in-situ forming implants with cabotegravir protect female macaques against rectal SHIV infection, Nat. Commun. 14 (2023) 708, https://doi.org/10.1038/s41467-023-36330-5.
[24] I.C. Young, A. Pallerla, M.L. Cottrell, P. Maturavongsadit, A. Prasher, R. Shrivastava, G.D. la Cruz, S.A. Montgomery, A. Schauer, C. Sykes, A.D. M. Kashuba, S.R. Benhabbour, Long-acting injectable multipurpose prevention technology for prevention of HIV and unplanned pregnancy, J. Control. Release 363 (2023) 606–620, https://doi.org/10.1016/j.jconrel.2023.10.006.
[25] M. Parent, C. Nouvel, M. Koerber, A. Sapin, P. Maincent, A. Boudier, PLGA in situ implants formed by phase inversion: critical physicochemical parameters to modulate drug release, J. Control. Release 172 (2013) 292–304, https://doi.org/10.1016/j.jconrel.2013.08.024.
[26] P. Schnabel, G.S. Merki-Feld, A. Malvy, I. Duijkers, E. Mommers, M.W. van den Heuvel, Bioequivalence and X-ray visibility of a radiopaque Etonogestrel implant versus a non-radiopaque implant, Clin. Drug Investig. 32 (2012) 413–422, https://doi.org/10.2165/11631930-000000000-00000.
[27] H.L.O. Júnior, B. Duchemin, S. Azzaye, M.R.F. Soares, B. Schneider, C. H. Romoaldo, Radiopaque Polyurethanes Containing Barium Sulfate: A Survey on Thermal, Rheological, Physical, and Structural Properties, Polymers 16, 2024, p. 3086, https://doi.org/10.3390/polym16213086.
[28] D.J.D. A, P.F. T, Radiopaque Catheter. https://patents.google.com/patent/EP0624380A1/en, 1994.
[29] N.R. James, J. Philip, A. Jayakrishnan, Polyurethanes with radiopaque properties, Biomaterials 27 (2006) 160–166, https://doi.org/10.1016/j.biomaterials.2005.05.099.
[30] S.Y. Choi, W. Hur, B.K. Kim, C. Shasteen, M.H. Kim, L.M. Choi, S.H. Lee, C.G. Park, M. Park, H.S. Min, S. Kim, T.H. Choi, Y.B. Choy, Bioabsorbable bone fixation plates for X-ray imaging diagnosis by a radiopaque layer of barium sulfate and poly (lactic-co-glycolic acid), J. Biomed. Mater. Res. Part B Appl. Biomater. 103 (2015) 596–607, https://doi.org/10.1002/jbm.b.33235.
[31] S.M. Kurtz, M.L. Villarraga, K. Zhao, A.A. Edidin, Static and fatigue mechanical behavior of bone cement with elevated barium sulfate content for treatment of vertebral compression fractures, Biomaterials 26 (2005) 3699–3712, https://doi.org/10.1016/j.biomaterials.2004.09.055.
[32] X. Lin, N.N.A. Zouabi, L.E. Ward, Z. Zhen, M. Darji, F.K. Masese, D. Hargrove, A. O. Beringhs, R.M. Kasi, Q. Li, Q. Zhang, B. Qin, Y. Wang, M. Jay, H. Yuan, X. Lu, Implant dynamics, inner structure, and their impact on drug release of in situ forming implants uncovered through CT imaging, J. Control. Release 375 (2024) 802–811, https://doi.org/10.1016/j.jconrel.2024.09.045.
[33] P. Liu, O.D. Wulf, J. Laru, T. Heikkilä, B. van Veen, J. Kiesvaara, J. Hirvonen, L. Peltonen, T. Laaksonen, Dissolution studies of poorly soluble drug Nanosuspensions in non-sink conditions, AAPS PharmSciTech 14 (2013) 748–756, https://doi.org/10.1208/s12249-013-9960-2.
[34] J.B. Joiner, A. Prasher, I.C. Young, J. Kim, R. Shrivastava, P. Maturavongsadit, S. R. Benhabbour, Effects of drug physicochemical properties on in-situ forming implant polymer degradation and drug release kinetics, Pharm 14 (2022) 1188, https://doi.org/10.3390/pharmaceutics14061188.
[35] C. Hernandez, N. Gawlik, M. Goss, H. Zhou, S. Jeganathan, D. Gilbert, A.A. Exner, Macroporous acrylamide phantoms improve prediction of in vivo performance of in situ forming implants, J. Control. Release 243 (2016) 225–231, https://doi.org/10.1016/j.jconrel.2016.10.009.
[36] C. Manaspon, C. Hernandez, P. Nittayacharn, S. Jeganathan, N. Nasongkla, A. A. Exner, Increasing distribution of drugs released from in situ forming PLGA implants using therapeutic ultrasound, Ann. Biomed. Eng. 45 (2017) 2879–2887, https://doi.org/10.1007/s10439-017-1926-1.
[37] G. Mardirossian, M. Tagesson, P. Blanco, L.G. Bouchet, M. Stabin, H. Yoriyaz, S. Baza, M. Ljungberg, S.E. Strand, A.B. Brill, A new rectal model for dosimetry applications, J. Nucl. Med. : Off. Publ., Soc. Nucl. Med. 40 (1999) 1524–1531.
[38] D. Karunakaran, S.M. Simpson, J.T. Su, E. Bryndza-Tfaily, T.J. Hope, R. Veazey, G. Dobek, J. Qiu, D. Watrous, S. Sung, J.E. Chacon, P.F. Kiser, Design and testing of a Cabotegravir implant for HIV prevention, J. Control. Release 330 (2021) 658–668, https://doi.org/10.1016/j.jconrel.2020.12.024.
[39] T. Zhou, H. Su, P. Dash, Z. Lin, B.L.D. Shetty, T. Kocher, A. Szlachetka, B. Lamberty, H.S. Fox, L. Poluektova, S. Gorantla, J. McMillan, N. Gautam, R. L. Mosley, Y. Alnouti, B. Edagwa, H.E. Gendelman, Creation of a nanoformulated cabotegravir prodrug with improved antiretroviral profiles, Biomaterials 151 (2018) 53–65, https://doi.org/10.1016/j.biomaterials.2017.10.023.
[40] T.A. Kulkarni, A.N. Bade, B. Sillman, B.L.D. Shetty, M.S. Wojtkiewicz, N. Gautam, J.R. Hilaire, S. Sravanam, A. Szlachetka, B.G. Lamberty, B.M. Morsey, H.S. Fox, Y. Alnouti, J.M. McMillan, R.L. Mosley, J. Meza, P.L. Domanico, T.-Y. Yue, G. Moore, B.J. Edagwa, H.E. Gendelman, A year-long extended release nanoformulated cabotegravir prodrug, Nat. Mater. 19 (2020) 910–920, https://doi.org/10.1038/s41563-020-0674-z.